Preserved fluvial cross strata record bedform disequilibrium dynamics

Kate Leary[1] and Vamsi Ganti[1,2]

[1] Department of Geography, University of California Santa Barbara, Santa Barbara, CA, USA. learykcp@ucsb.edu

[2] Department of Earth Science, University of California Santa Barbara, Santa Barbara, CA, USA.

Contents of this file

Additional Supporting Information (Files uploaded separately)

Introduction

In this supplement, we summarize experimental details (text S1), provide further information on the methods used for computing the bedform migration and deformation rates (text S2), and estimating bedform turnover timescale and characteristic duration of flood recession in modern rivers (text S3). In addition, we have tabulated the bedform turnover timescales, characteristic duration of flood recession, bedform migration rates, bedform wavelengths, bedform heights, riverbed slopes, and bedload transport rates for modern rivers in Table S1, which was used to produce Figure 4d of the main text.

Text S1.
    All experiments reported here were conducted in the tilting flume at the St. Anthony Falls Laboratory, University of Minnesota, with the same configuration. Martin and Jerolmack (2013) conducted a series of seven experiments to assess the growth and decay processes of bedforms adjusting to changing flow conditions. Five of these experiments consisted of step changes (i.e. instantaneous increase or decrease) from low to high discharges and back to low discharges, with varying low and high discharge magnitudes (see Table 1 in Martin and

Jerolmack, 2013). They used these step-discharge experiments to quantify and validate the bedform turnover timescales for the growth and decay process of bedforms. Further, they conducted two experiments in which discharge was increased incrementally from 0.04 m³/s to 0.115 m³/s (every 5 minutes for the fast flood and every 20 minutes for the slow flood) producing a triangular flood wave (Fig. S1). Conceptually, these experiments represent natural rivers with broad and flashy hydrographs, and we analyzed these two experiments in our study.

We used steady-state experiments conducted in the same flume as a control. Ganti et al. (2013) studied bedform evolution for two steady-state experimental runs with a water discharge magnitude of 0.04 m³/s and 0.08 m³/s. We chose the 0.08 m³/s experiment as a control for our triangular flood wave analyses because it represents bedform evolution equilibrated to the mean discharge of the flood wave experiments. In addition, we also measured the bedform preservation ratio, and coefficient of variation of preserved set thickness for the steady state experiment with a constant discharge of 0.04 m³/s (Ganti et al., 2013).

We refer the readers to the original publications for detailed description of the experimental setup, data collection apparatus, and details about the evolution of bedform geometry. All these experimental datasets are freely available at the Sediment Experimentalist Network's data repository.

Text S2.

We computed bedform migration and deformation rates (equation 3 in main text) using well-established methods. Bedform migration rates were calculated by cross-correlating successive bed elevation profiles following the method of McElroy and Mohrig (2009). The calculated maximum lag between the profiles denotes the characteristic distance traveled by the bedforms. Bedform migration rate was then equated to the ratio of this lag distance and the time difference between the bed profiles. We note our computations yield one characteristic bedform migration rate for the entire bed profile at each timestep, which effectively denotes the bed velocity of the entire profile. We did not compute the bedform migration rate of individual bedforms because superimposed bedform migration results in changes in shape of the host bedforms, which corresponds to the localized changes in sedimentation and erosion rates that significantly effect cross-stratal preservation. Our estimated bedform migration rates are similar to those documented by Martin and Jerolmack (2013) for the unsteady experiments. They used a different approach where they created space-time plots of dune crestlines and computed the slopes of continuous crestlines in this phase space.

Once we computed the bedform migration rates for each timestep for all experiments, we computed the deformation rates using a discretized version of equation (3) (McElroy and Mohrig, 2009). This is similar to computing elevation differences in a Lagrangian framework where the later-time bed profile is shifted upstream by the distance that corresponds to the maximum lag and then differenced with the earlier-time bed profile. Figures S2 and S3 show the bedform migration and deformation rates through time for both the fast and slow flood runs. Figure S4 shows bedform profiles in the Lagrangian reference frame for the fast, slow, and steady state runs.

Text S3.

Bedform turnover timescales were calculated following equation (1) in the main text:

$$T_t = \lambda h_d \beta / q_s \quad \text{(S1)}$$

We used Simons et al. (1965) relation to estimate unit sediment flux, which resulted in an expression for the bedform turnover timescale, given by:

$$T_t = \frac{\lambda h_d \beta}{(1-p)V_c h_d/2} \quad \text{(S2)}$$

where p is the bed porosity (assumed here to be ~0.5). We also assume a bedform shape factor (β) of approximately 0.5, consistent with both experimental and field observations (Simons et al., 1965; van den Berg, 1987; Ten Brinke et al., 1999; Venditti et al., 2005). Thus, equation (S2) can be simplified to:

$$T_t = \frac{2\lambda}{V_c} \quad \text{(S3)}$$

For steady-state experiments, we used the reported values of bedform wavelength and migration rates from Ganti et al. (2013) to estimate the bedform turnover timescale. Ganti et al. (2013) reported bedform migration timescales (i.e. the average timescale it takes bedforms to migrate the average bedform wavelength) of 41.2 minutes and 20.8 minutes for the steady experiments with a water discharge of 0.04 m^3/s and 0.08 m^3/s experiments, respectively.

To compute the bedform turnover timescales for modern rivers, we either used equation (S1) or (S3), contingent upon the availability of data (Table S1). For rivers where only the bedform geometries were reported, we used the empirical relationship between bedform migration rate and channel slope proposed by Mahon and McElroy (2018) to approximate V_c, and consequently the bedform turnover timescale (equation S3).

Finally, we computed the characteristic duration of flood recession primarily from historical daily water discharge records, compiled from the Global Runoff Data Centre, 56068 Koblenz, Germany. In some cases, we used higher resolution flood discharge data when available, and this is noted in Table S1. The following workflow was adopted to estimate the characteristic duration of flood recession (Fig. S5):
  a) Every time series of discharge data was normalized by the mean annual discharge for the given year of record. When data were available for multiple years, we performed this operation individually on every year's dataset for a given river.
  b) Flood events were identified as times in the year when the normalized discharge was greater than 1 (i.e. instantaneous flow greater than mean annual flow; Figure S5).
  c) We then computed the average, continuous time for which the normalized discharge was greater than 1, which characterizes the typical flood hydrograph duration for each river.
  d) Finally, we divided this duration by 2 to represent the average timescale of flood recession, analogous to experimental flood waves.

Because the duration of flood recession had a skewed distribution, we reported their interquartile ranges to better characterize the spread in the data.

We note that theoretical prediction of T^* < 1 leading to bedform hysteresis was independently corroborated for multiple rivers in our dataset, which provides further support for that Figure

4d adequately characterizes the nature of bedform evolution in unsteady flows for extant rivers.

Supplementary References

Allen, J. R. L. (1976). Time-lag of dunes in unsteady flows: an analysis of Nasner's data from the R. Weser, Germany. Sedimentary Geology, 15(4), 309–321.

Almeida, R. P. de, Galeazzi, C. P., Freitas, B. T., Janikian, L., Ianniruberto, M., & Marconato, A. (2016). Large barchanoid dunes in the Amazon River and the rock record: Implications for interpreting large river systems. Earth and Planetary Science Letters, 454, 92–102. https://doi.org/10.1016/j.epsl.2016.08.029

Claude, N., Rodrigues, S., Bustillo, V., Bréhéret, J. G., Macaire, J. J., & Jugé, P. (2012). Estimating bedload transport in a large sand-gravel bed river from direct sampling, dune tracking and empirical formulas. Geomorphology, 179, 40–57.

Coleman, J. M. (1969). Brahmaputra River: channel processes and sedimentation. Sedimentary Geology, 3(2–3), 129–239.

Gabel, S. L. (1993). Geometry and kinematics of dunes during steady and unsteady flows in the Calamus River, Nebraska, USA. Sedimentology, 40(2), 237–269.

Harvey, J. W., Drummond, J. D., Martin, R. L., McPhillips, L. E., Packman, A. I., Jerolmack, D. J., et al. (2012). Hydrogeomorphology of the hyporheic zone: Stream solute and fine particle interactions with a dynamic streambed. Journal of Geophysical Research: Biogeosciences, 117(G4). https://doi.org/10.1029/2012JG002043

Holmes, R. R., & Garcia, M. H. (2008). Flow over bedforms in a large sand-bed river: A field investigation. Journal of Hydraulic Research, 46(3), 322–333. https://doi.org/10.3826/jhr.2008.3040

Kleinhans, M. G., & Brinke, W. B. T. (2001). Accuracy of cross-channel sampled sediment transport in large sand-gravel-bed rivers. Journal of Hydraulic Engineering, 127(4), 258–269.

Leary, K. C. P., & Buscombe, D. (2019). Estimating Sand Bedload in Rivers by Tracking Dunes: a comparison of methods based on bed elevation time-series. Earth Surface Dynamics Discussions, 1–16. https://doi.org/10.5194/esurf-2019-38

Mohrig, D., & Smith, J. D. (1996). Predicting the migration rates of subaqueous dunes. Water Resources Research, 32(10), 3207–3217.

Nittrouer, J. A., Allison, M. A., & Campanella, R. (2008). Bedform transport rates for the lowermost Mississippi River. Journal of Geophysical Research: Earth Surface, 113(F3). https://doi.org/10.1029/2007JF000795

Nordin, C., & Perez-Hernandez, D. (1989). The Waters and Sediments of the Rio Orinoco and its Major Tributaries, Venezuela and Colombia. Chap. A, Sand Waves, Bars and Wind-Blown Sands of the Rio Orinoco, Venezuela and Colombia, USGS Water-Supply Paper A, 2326, A1–A74.

Parsons, D., Best, J., Orfeo, O., Hardy, R., Kostaschuk, R., & Lane, S. (2005). Morphology and flow fields of three-dimensional dunes, Rio Paraná, Argentina: Results from simultaneous multibeam echo sounding and acoustic Doppler current profiling. Journal of Geophysical Research: Earth Surface, 110(F4).

Peters, J. J. (1978). Discharge and sand transport in the braided zone of the Zaire estuary. Netherlands Journal of Sea Research, (3–4).

Simons, D.B., Richardson, E.V. and Nordin, C.F. (1965) Bedload equation for ripples and dunes. U.S. Geol. Surv. Prof. Pap., 462-H, 1–9.

Smith, G. H. S., Ashworth, P. J., Best, J. L., Lunt, I. A., Orfeo, O., & Parsons, D. R. (2009). The Sedimentology and Alluvial Architecture of a Large Braid Bar, Río Paraná, Argentina. Journal of Sedimentary Research, 79(8), 629–642. https://doi.org/10.2110/jsr.2009.066

Sukhodolov, A. N., Fedele, J. J., & Rhoads, B. L. (2006). Structure of flow over alluvial bedforms: an experiment on linking field and laboratory methods. Earth Surface Processes and Landforms, 31(10), 1292–1310. https://doi.org/10.1002/esp.1330

Ten Brinke, W.B.M., Wilbers, A.W.E. and Wesseling, C. (1999) Dune growth, decay and migration rates during a large- magnitude flood at a sand and mixed-gravel bed in the Dutch Rhine river system. In: Fluvial Sedimentology VI (Eds N.D. Smith and J. Rogers), Spec. Publ. Int. Assoc. Sedimentol., 28, pp. 15–32. Blackwell Science, Malden, MA.

Unsworth, C. A. (2015). River dunes in unsteady conditions (Ph.D.). University of Hull. Retrieved from http://hydra.hull.ac.uk/resources/hull:13096

van den Berg, J.H. (1987) Bedform migration and bed-load transport in some rivers and tidal environments. Sedimentology, 34, 681–698.

Venditti, J. G., & Bauer, B. O. (2005). Turbulent flow over a dune: Green River, Colorado. Earth Surface Processes and Landforms, 30(3), 289–304.

Venditti, J.G., Church, M. and Bennett, S.J. (2005) Morphodynamics of small-scale superimposed sand waves over migrating dune bed forms. Water Resour. Res., 41, W10423. doi:10.1029/2004WR003461.

Villard, P. V., & Church, M. (2003). Dunes and associated sand transport in a tidally influenced sand-bed channel: Fraser River, British Columbia. Can. J. Earth Sci., 40(1), 115–130.

Wilbers, A. W. E., & Ten Brinke, W. B. M. (2003). The response of subaqueous dunes to floods in sand and gravel bed reaches of the Dutch Rhine. Sedimentology, 50, 1013–1034.
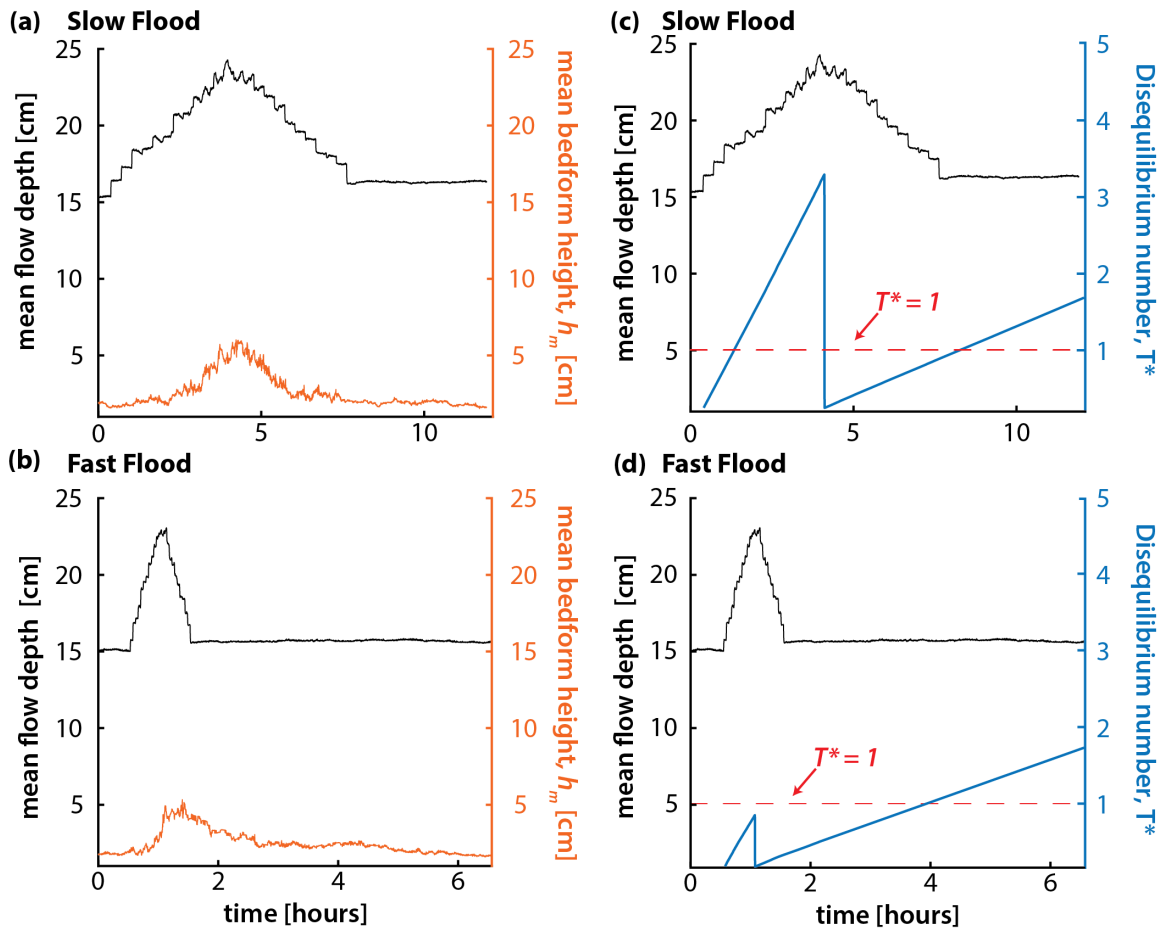
Figure S1. Changes in spatially-averaged flow depth and mean bedform height through time for the (a) slow and (b) fast floods. Changes in spatially-averaged flow depth and bedform disequilibrium number through time for the (c) slow and (d) fast floods.
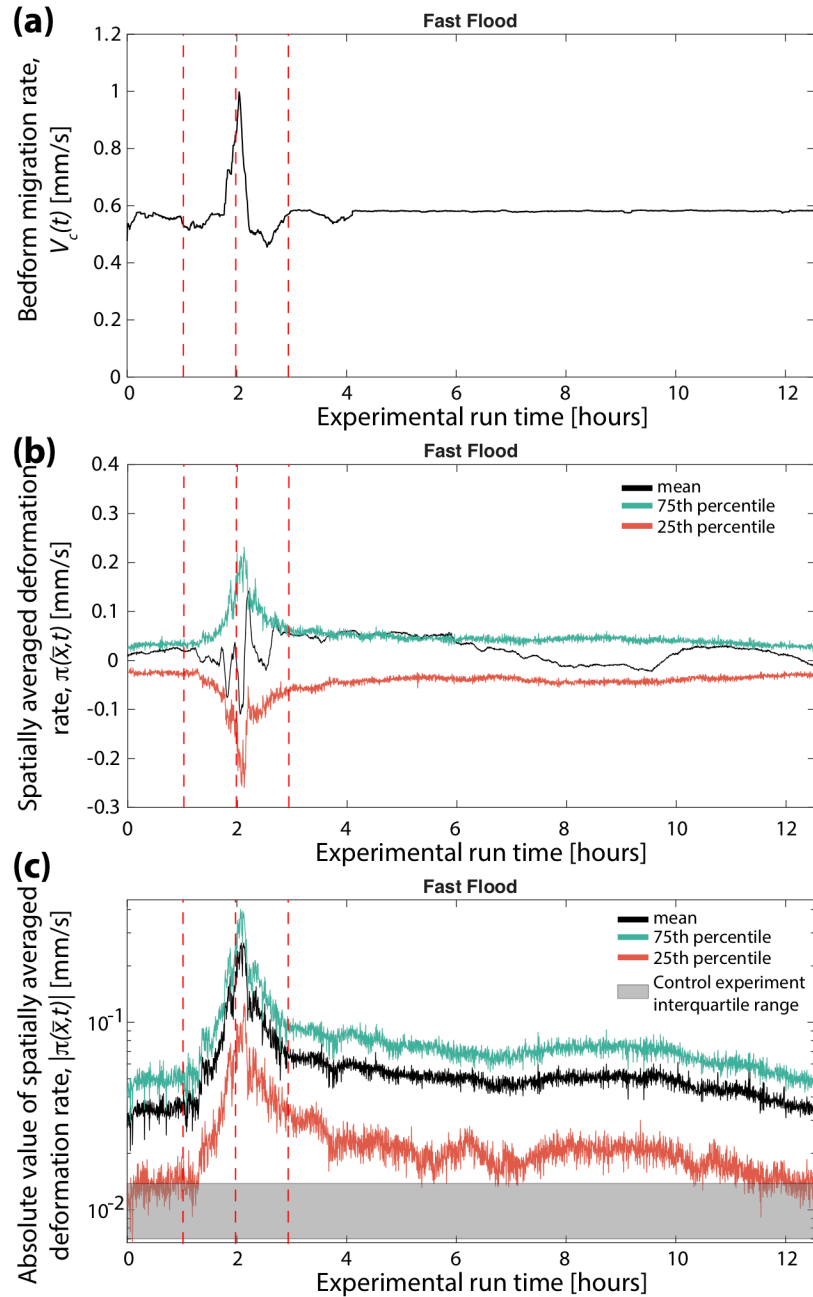
Figure S2. Estimated bedform migration and deformation rates through time for the fast flood. Temporal evolution of (a) bedform migration rates, (b) spatially-averaged bedform deformation rate, and (c) absolute value of spatially-averaged bedform deformation rates. Red dashed lines indicate the beginning, peak, and end of the flood event.
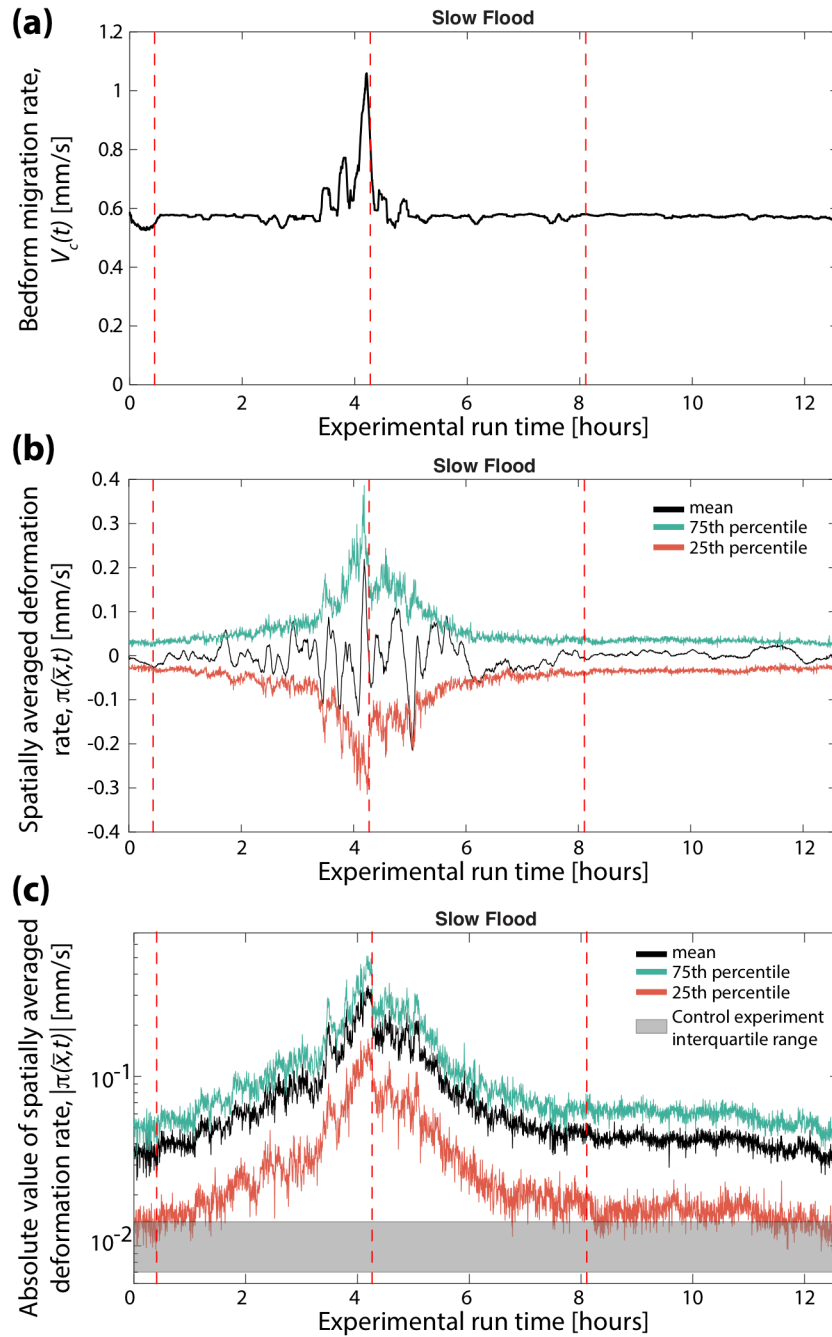
Figure S3. Estimated bedform migration and deformation rates through time for the slow flood. Temporal evolution of (a) bedform migration rates, (b) spatially-averaged bedform deformation rate, and (c) absolute value of spatially-averaged bedform deformation rates. Red dashed lines indicate the beginning, peak, and end of the flood event.
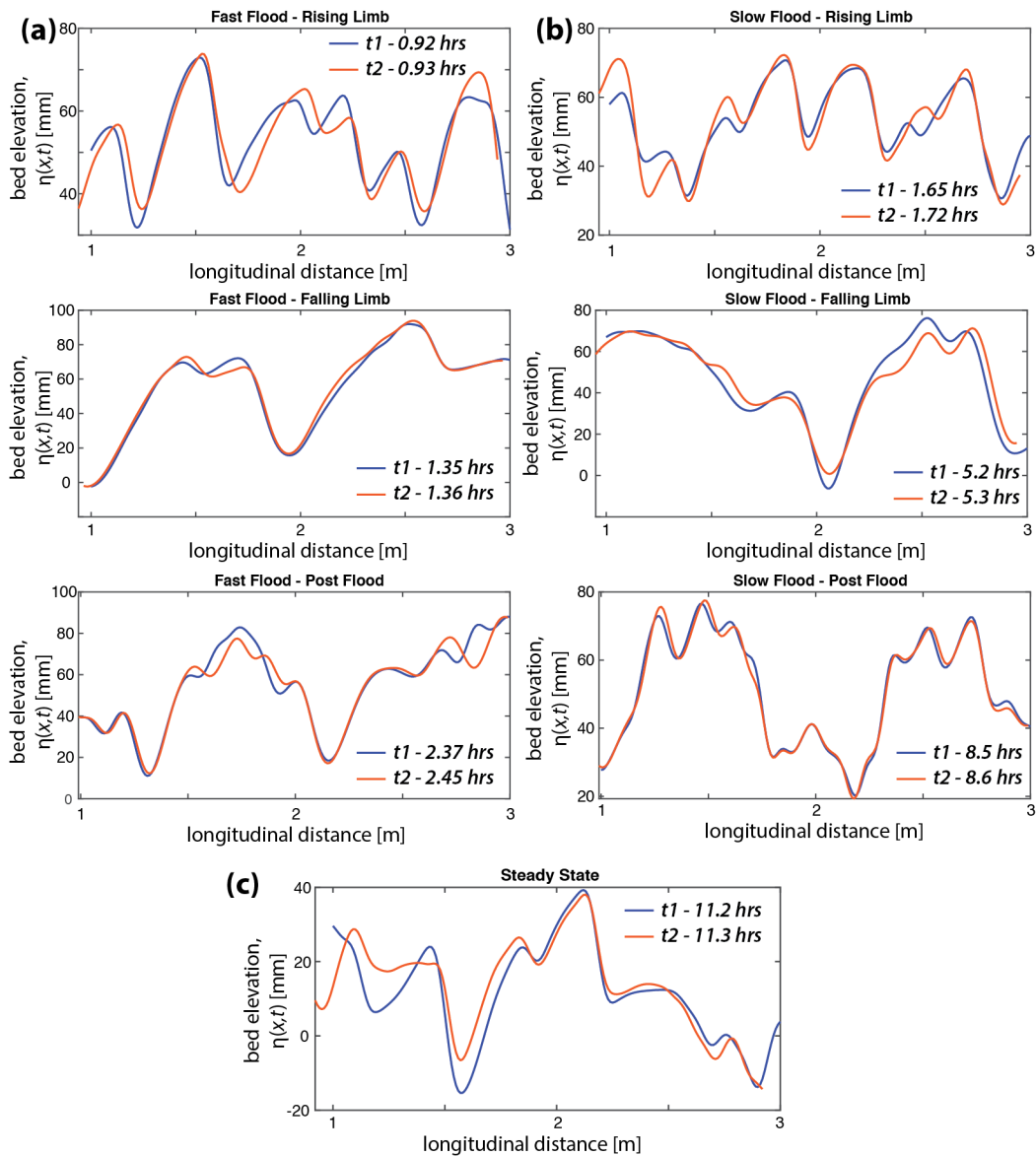
Figure S4. Bed elevation profiles in the Lagrangian reference frame for the (a) fast flood, (b) slow flood, and (c) steady state experimental runs. Notice that preservation in unsteady flows is centered around the peaks and body of the bedforms; however, preservation in steady-state experiment occurs via variable bed scours, resulting from bedform troughs.
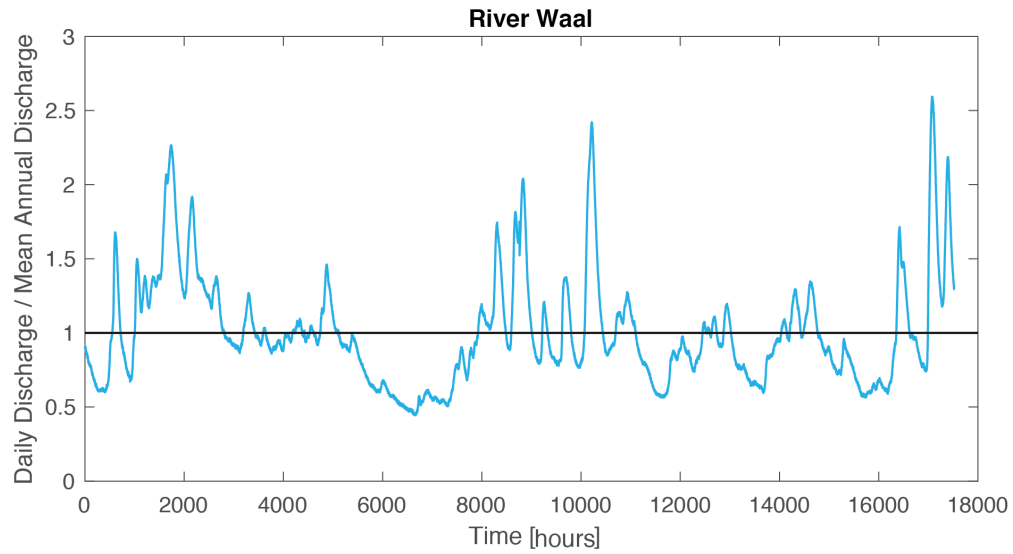
Figure S5. Daily discharge normalized by mean annual discharge for the River Waal over a period of two years.

Table S1. Bedform geometries, turnover timescales, and representative flood recession timescales for modern rivers.